

IL-15 promotes activation and expansion of CD8⁺ T cells in HIV-1 infection

Souheil-Antoine Younes,¹ Michael L. Freeman,¹ Joseph C. Mudd,² Carey L. Shive,¹ Arnold Reynaldi,³ Soumya Panigrahi,¹ Jacob D. Estes,⁴ Claire Deleage,⁴ Carissa Lucero,⁴ Jodi Anderson,⁵ Timothy W. Schacker,⁵ Miles P. Davenport,³ Joseph M. McCune,⁶ Peter W. Hunt,⁷ Sulggi A. Lee,⁷ Sergio Serrano-Villar,⁸ Robert L. Debernardo,⁹ Jeffrey M. Jacobson,¹⁰ David H. Canaday,¹ Rafick-Pierre Sekaly,¹¹ Benigno Rodriguez,¹ Scott F. Sieg,¹ and Michael M. Lederman¹

¹Center for AIDS Research, Department of Medicine, Case Western Reserve University and University Hospitals, Case Medical Center, Cleveland, Ohio, USA. ²Immunopathogenesis Section, Laboratory of Parasitic Diseases, National Institute of Allergy and Infectious Diseases, NIH, Bethesda, Maryland, USA. ³Kirby Institute for Infection and Immunity, University of New South Wales, Sydney, New South Wales, Australia. ⁴AIDS and Cancer Virus Program, Leidos Biomedical Research Inc., Frederick National Laboratory for Cancer Research, Frederick, Maryland, USA. ⁵Department of Medicine, University of Minnesota, Minneapolis, Minnesota, USA. ⁶Division of Experimental Medicine and ⁷HIV/AIDS Division, Department of Medicine, UCSF, San Francisco, California, USA. ⁸Department of Infectious Diseases, University Hospital Ramón y Cajal, Madrid, Spain. ⁹Lerner College of Medicine, Cleveland Clinic, Cleveland, Ohio, USA. ¹⁰Lewis Katz School of Medicine, Temple University, Philadelphia, Pennsylvania, USA. ¹¹Department of Pathology, Case Western Reserve University, Cleveland, Ohio, USA.

In HIV-1-infected patients, increased numbers of circulating CD8⁺ T cells are linked to increased risk of morbidity and mortality. Here, we identified a bystander mechanism that promotes CD8 T cell activation and expansion in untreated HIV-1-infected patients. Compared with healthy controls, untreated HIV-1-infected patients have an increased population of proliferating, granzyme B⁺, CD8⁺ T cells in circulation. Vβ expression and deep sequencing of CDR3 revealed that in untreated HIV-1 infection, cycling memory CD8 T cells possess a broad T cell repertoire that reflects the repertoire of the resting population. This suggests that cycling is driven by bystander activation, rather than specific antigen exposure. Treatment of peripheral blood mononuclear cells with IL-15 induced a cycling, granzyme B⁺ phenotype in CD8⁺ T cells. Moreover, elevated IL-15 expression in the lymph nodes of untreated HIV-1-infected patients correlated with circulating CD8⁺ T cell counts and was normalized in these patients following antiretroviral therapy. Together, these results suggest that IL-15 drives bystander activation of CD8⁺ T cells, which predicts disease progression in untreated HIV-1-infected patients and suggests that elevated IL-15 may also drive CD8⁺ T cell expansion that is linked to increased morbidity and mortality in treated patients.

Introduction

An unexplained characteristic of untreated HIV-1 infection is sustained expansion of circulating CD8⁺ T cell numbers that has been associated with increased CD8⁺ T cell activation, cycling, and turnover (1–3). The drivers of CD8⁺ T cell activation and expansion are not clearly defined, and, importantly, CD8⁺ T cell expansion is linked to an increased risk of morbidity and mortality during treated HIV-1 infection (4–7). While expansion of CD8⁺ T cells in response to HIV-1 peptides is demonstrable in early infection, it is unlikely that expansion of HIV-1-reactive cells constitutes the bulk of the CD8⁺ T cell expansion. In chronic infection, for example, only 1%–18% of circulating CD8⁺ T cells are demonstrably HIV-1-reactive (8–10), while the proportion of circulating CD8⁺ T cells expressing activation markers such as CD38 and HLA-DR may exceed 60% (11, 12), and CD8⁺ T cell numbers in circulation are typically expanded severalfold (2, 3, 9, 11, 13, 14).

We have provided evidence recently that the increased cycling of memory CD4⁺ T cells in viremic HIV-1-infected patients appears to be largely the consequence of bystander

activation (15). CD8⁺ T cell activation predicts the course of disease during untreated infection (4–7), and CD8⁺ T cell expansion predicts the course of treated HIV-1 infection (13). We show here that memory CD8⁺ T cells are frequently cycling in untreated HIV-1 infection and that the T cell receptor repertoire of the cycling cells is tightly linked to the T cell receptor repertoire of the resting memory CD8⁺ T cell compartment. Despite this, in HIV-1 infection, but not in healthy controls, cycling is particularly enriched among memory cells with specificities for viral peptides, regardless of peptide prevalence. In addition, CD8⁺ T cells with specificities for both prevalent and nonprevalent microbial peptides are enriched for expression of granzyme B in HIV-1 infection. This phenotype of CD8⁺ T cell cycling and granzyme B expression can be reproduced in vitro by exposure to IL-15. IL-15 protein expression is increased in the lymph nodes of untreated HIV-1-infected patients, and suppression of HIV-1 replication by antiretroviral therapy (ART) normalizes IL-15 levels. In contrast to findings among healthy individuals and ART-treated subjects, lymph node IL-15 levels in untreated HIV-1 infection are correlated with circulating CD8⁺ T cell numbers. These data suggest that IL-15 may drive the dramatic bystander expansion and functional differentiation of CD8⁺ T cells in chronic HIV-1 infection.

Conflict of interest: The authors have declared that no conflict of interest exists.

Submitted: December 11, 2015; **Accepted:** May 4, 2016.

Reference information: *J Clin Invest.* 2016;126(7):2745–2756. doi:10.1172/JCI185996.

Table 1. Patients in whom peripheral CD8 T cell responses were assessed

	<i>n</i>	Age ^A	Gender	ART	Plasma HIV-1 RNA ^B	CD4 ^C	CD8 ^D	Class I haplotype
Healthy controls	9	35 (27–45)	7 male, 2 female	Negative	NA	805 (720–1,001)	420 (350–654)	HLA-A*02:01
HIV1 ⁺ untreated	20	42 (29–55)	15 male, 5 female	Negative	210,000 (50,000–420,000)	414 (341–611)	780 (585–1100)	HLA-A*02:01
Immune success	12	40 (26–57)	9 male, 3 female	Positive	<50	610 (449–830)	700 (601–951)	ND
Immune failure	10	45 (30–54)	8 male, 2 female	Positive	<50	249 (180–308)	704 (660–940)	ND
Healthy elderly	10	75 (70–80)	10 male	Negative	NA	731 (701–920)	433 (398–602)	ND

^AMedian age (min.–max.); ^Bmedian plasma HIV-1 RNA (min.–max.); ^Cmedian peripheral CD4 T cell count (min.–max.); ^Dmedian peripheral CD8 T cell count (min.–max.). NA, not applicable; ND, not determined.

Results

The proportion of Ki-67⁺ cycling CD8⁺ T cells is increased during untreated HIV-1 infection, and cycling cells are primarily within the CCR7⁺CD45RO⁺ effector memory subset. We and others have previously demonstrated an increased cycling of CD8⁺ T cells in untreated HIV-1 infection (2, 3, 9, 11, 14). We compared the frequency of cycling in untreated HIV-1 infection, healthy controls, healthy elderly patients, and HIV-1-infected patients receiving suppressive ART who either normalized circulating CD4 T cells (“immune successes”) or did not increase circulating CD4 T cells to levels greater than 350/μl (“immune failures”). Patient characteristics are shown in Table 1.

As shown in Figure 1A, the proportion of CD8⁺ T cells in cell cycle is dramatically expanded in viremic HIV-1 infection with a median of 16% of CD8⁺ T cells being Ki-67⁺. In contrast, healthy controls, elderly healthy controls, and HIV-1-infected patients in whom viremia was suppressed by ART, whether immune successes or immune failures, had much lower frequencies of circulating CD8⁺ T cells in cycle, averaging approximately 2% in each group. In viremic HIV-1 infection, Ki-67⁺ cells were especially enriched in the effector memory (CD45RO⁺CCR7⁺) subset (Figure 1, B and C). The expanded CD8⁺ T cells in HIV-1-infected patients are mainly effector memory cells, and these expanded cells frequently express granzyme B (Figure 1D).

Cycling memory CD8⁺ T cells exhibit a broad T cell receptor repertoire during untreated HIV-1 disease. We hypothesized that if cycling were largely a consequence of antigen-driven expansion of memory cells during untreated HIV-1 infection, we might see a skewing of the T cell receptor repertoire among the cycling cells. We therefore compared the Vβ distribution of Ki-67⁺ CD45RO⁺ CD8⁺ T cells to the Vβ distribution among Ki-67⁺ CD45RO⁺ CD8⁺ T cells of healthy donors (*n* = 6) and untreated HIV-1-infected patients (*n* = 9) using a panel of monoclonal antibodies that identifies approximately 70% of the T cell receptor Vβ repertoire. Figure 2A shows representative panels reflecting the Vβ distribution among Ki-67⁺ and Ki-67⁺ CD45RO⁺ CD8⁺ T cells from an untreated HIV-1-infected patient. We hypothesized that if cycling were driven by bystander mechanisms, dividing memory cells would represent a random selection of the total memory CD8⁺ T cell population. Thus their Vβ repertoires would be similar. On the other hand, if cycling were driven largely by exposure to prevalent antigens, we would expect that the Ki-67⁺ CD8⁺ T cells would have a Vβ repertoire distinguishable from the repertoire of the resting memory CD8⁺ T cell population. We found that in untreated HIV-1⁺ individuals, the distribution of

Vβ expression of Ki-67⁺ cells was actually better correlated to the Vβ distribution of the Ki-67⁺ cells than was seen among healthy controls (Figure 2B; mean Spearman *r* value = 0.94 vs. 0.90, *P* = 0.0048, Mann-Whitney). One possible explanation for the slightly stronger correlation in HIV-1 infection is that the memory CD8⁺ T cell repertoire often tends to greater representation of certain Vβ families in both the Ki-67⁺ and Ki-67⁺ memory compartment, as has been seen in some (16, 17) but not all studies (18).

To analyze further the diversity of proliferating and non-proliferating memory CD8 T cells, cycling and noncycling CD45RO⁺CCR7⁺ CD8⁺ T cells from 3 HIV-1 viremic and 3 healthy uninfected subjects were FACS-sorted, and 60,000 purified cells from each population were lysed and CDR3 segments were sequenced. Cycling and noncycling cells were distinguished by surface expression of CD71, the transferrin receptor that is a near-perfect marker of cells expressing intracellular Ki-67 (Supplemental Figure 1; supplemental material available online with this article; doi:10.1172/JCI85996DS1). As shown in Figure 2C, the distribution of CDR3 sequences among cycling effector memory CD8⁺ T cells reflected the distribution of CDR3 sequences among the resting effector memory CD8⁺ T cell population in both healthy controls and viremic HIV-1-infected people. Sequence diversity of these populations as measured by the Shannon entropy calculation (see Methods) was similar in cycling and noncycling populations of patients and controls (Figure 2D).

Thus, by both Vβ expression and deep sequencing of the CDR3 region, the T cell receptor diversity of cycling effector memory CD8⁺ T cells reflects the clonal diversity of the entire CD8⁺ effector memory population in health and in untreated HIV-1 infection. If bursts of antigen-driven activation and cycling are occurring in untreated HIV infection, they are occurring below the limits of our ability to detect them and the vast majority of CD8⁺ T cell cycling in untreated HIV infection (and in health) appears to be driven by bystander mechanisms.

Memory CD8⁺ T cells reactive with viral peptides are more frequently cycling in untreated HIV-1 infection irrespective of antigen prevalence. As memory CD8⁺ T cell cycling appeared to be driven largely by bystander mechanisms, we examined the binding of MHC class I HLA-A*02:01 tetramers that detect CD8⁺ T cells specific for a short-lived viral infection (influenza) or for persistent viral infections (CMV and HIV-1). Among healthy controls, the cycling frequency among effector memory (CD45RO⁺CCR7⁺) CD8⁺ T cells that bound either influenza or CMV peptide-tetramer complexes was similar to or lower than the cycling fre-

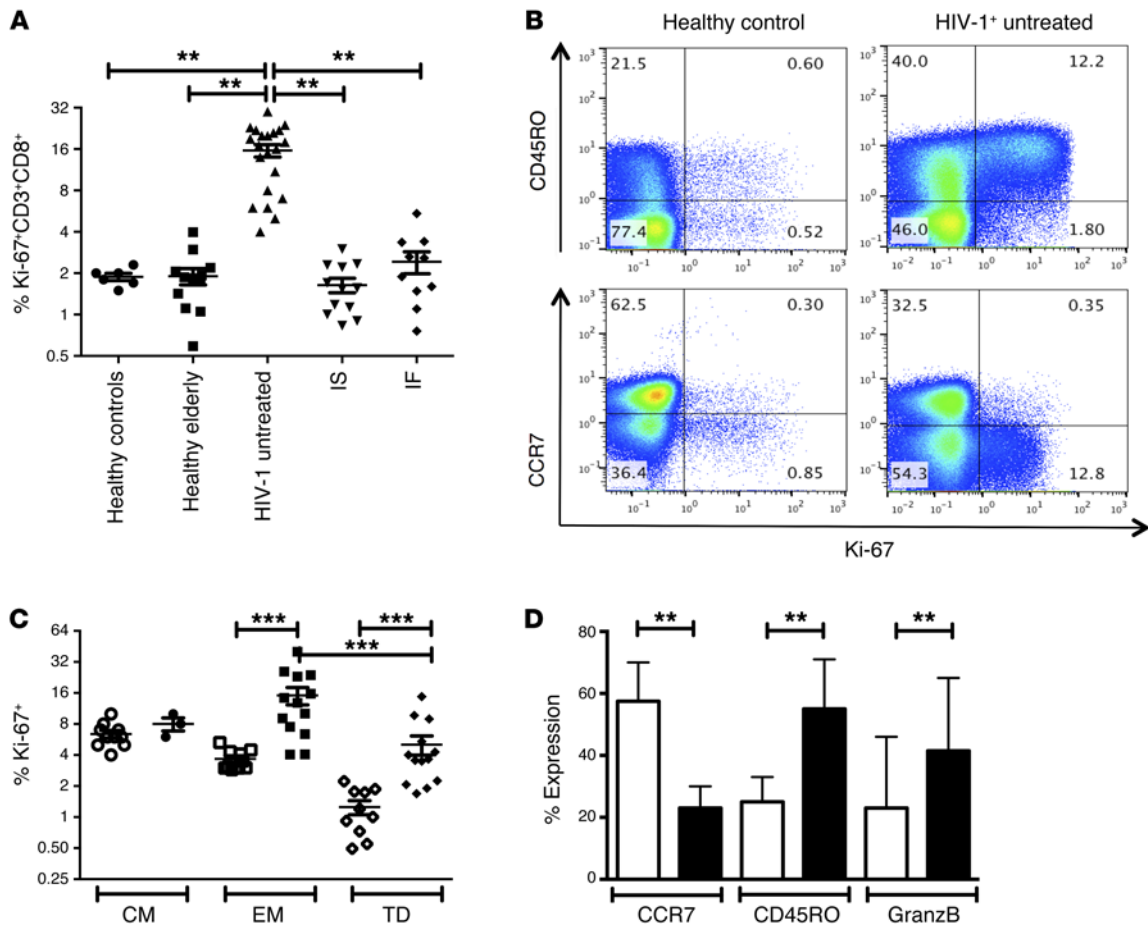


Figure 1. Increased cycling of CD45RO⁺ CD8⁺ T cells in viremic HIV-1 infection. (A) Percentages of Ki-67⁺ CD3⁺ CD8⁺ cells among healthy donors ($n = 7$), healthy elderly donors ($n = 10$), HIV-1⁺ viremic subjects ($n = 20$), ART-treated immune success (IS) patients ($n = 12$), and ART-treated immune failure (IF) ($n = 10$) patients. (B) Representative dot plots showing that Ki-67⁺ CD8⁺ cells are predominantly found within the CD45RO⁺ CCR7⁻ effector memory-phenotype CD8⁺ T cell subset. (C) Proportions of cycling Ki-67⁺ CD8⁺ T cells in central (CM) (CCR7⁺ CD45RO⁺), effector (EM) (CCR7⁻ CD45RO⁺), and terminally differentiated (TD) (CCR7⁻ CD45RO⁻) memory populations in 7 healthy controls (white symbols) and 13 HIV-1-infected viremic patients (black symbols). (D) Expression of CCR7, CD45RO, and granzyme B among total peripheral blood CD8⁺ T cells in healthy controls ($n = 7$, white bars) and HIV-1-infected viremic patients ($n = 20$, black bars). ** $P < 0.01$, *** $P < 0.001$ by Kruskal-Wallis test.

quency among all effector memory CD8⁺ T cells (Figure 3A). In contrast and perhaps not surprisingly, in untreated HIV-1 infection, the cycling of effector memory CD8⁺ T cells binding CMV and HIV-1 peptide-tetramer complexes was significantly greater than among the total effector memory CD8⁺ T cell population (median 25% of CMV peptide-tetramer-binding and 30% of HIV peptide-tetramer-binding effector memory CD8⁺ T cells were Ki-67⁺ vs. 16% of total effector memory CD8⁺ T cells, $P < 0.01$) (Figure 3B). This may reflect the sustained or intermittent exposure of these cells to peptides derived from these replicating viruses. To our surprise, however, the cycling of effector memory CD8⁺ T cells binding influenza peptide-tetramer complexes was also significantly greater than among the total effector memory CD8⁺ T cell population (median 35% vs. 16%, $P = 0.0022$), although many of these samples (8 of 20) were obtained during seasons when influenza exposure was unlikely. A representative flow cytometry result from an untreated patient sample is shown in Figure 3C demonstrating both an expected greater proportion of cycling cells in the effector memory

(CD45RO⁺ CCR7⁻) population than among the terminally differentiated (CD45RO⁻ CCR7⁺) population and increased cycling among cells reactive with peptides of HIV-1, CMV, and influenza.

Thus while our studies of repertoire diversity suggest that bystander mechanisms rather than ongoing exposure to antigen are driving CD8 T cell cycling in untreated HIV-1 infection, cells with memory of viral peptide exposure may be particularly prone to cycling irrespective of the persistence of antigen.

Memory CD8⁺ T cells reactive with viral peptides are enriched for granzyme B in untreated HIV-1 infection, even in the absence of antigen. To explore further the characteristics of memory CD8⁺ T cells in HIV-1 infection, we examined the expression of granzyme B in peptide-tetramer-reactive cells, reasoning that persistent viral infections such as CMV or HIV-1 sustain continuous CD8⁺ T cell stimulation. By contrast, influenza-reactive CD8⁺ T cells would be expected to transition into a resting state once virus is cleared during the course of self-limited infection. In healthy controls, most influenza-specific CD8⁺ T cells are in the granzyme B⁻ subset whereas, on average, approximately 70% of CMV peptide-binding CD8⁺

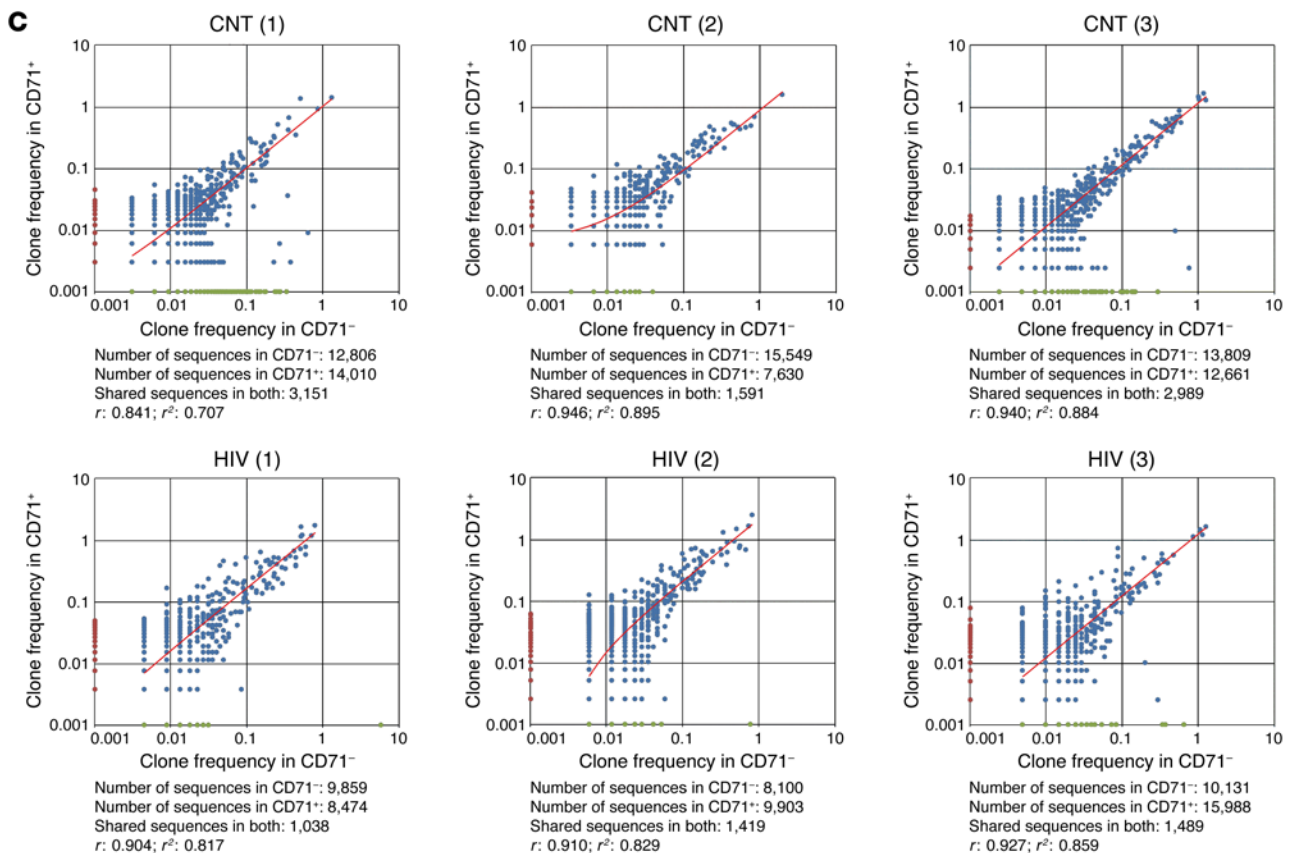
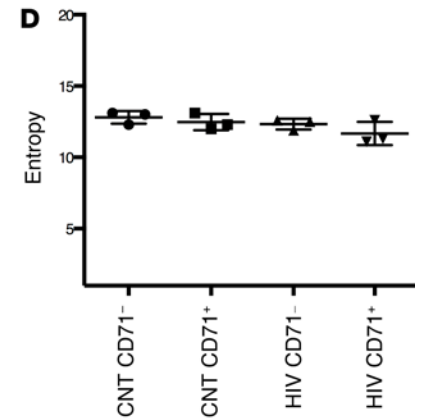
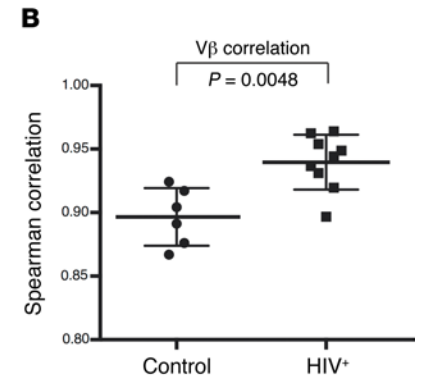
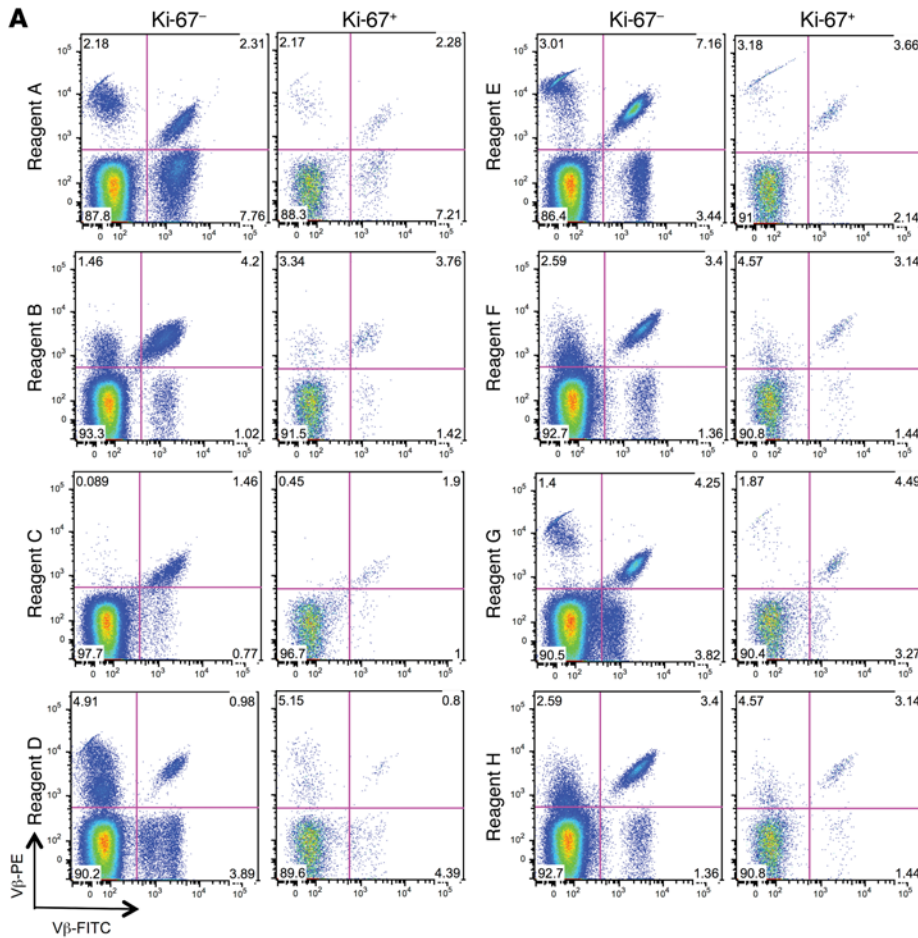


Figure 2. T cell receptor V β family distributions and CDR3 sequencing among cycling and noncycling memory CD8⁺ T cells. (A) CD45RO⁺ CD8⁺ T cells from a viremic HIV-1-infected patient were stained with reagents A to H having combinations of 3 anti-V β antibodies—A (V β 5.3-PE, V β 7.1-PE-FITC, V β 3-FITC), B (V β 9-PE, V β 17-PE-FITC, V β 16-FITC), C (V β 18-PE, V β 5.1-PE-FITC, V β 20-FITC), D (V β 13.1-PE, V β 13.6-PE-FITC, V β 8-FITC), E (V β 5.2-PE, V β 2-PE-FITC, V β 12-FITC), F (V β 23-PE, V β 1-PE-FITC, V β 21.3-PE), G (V β 11-PE, V β 22-PE-FITC, V β 14-FITC), and H (V β 13.2-PE, V β 4-PE-FITC, V β 7.2-FITC)—and enumerated according to intracellular staining for Ki-67 as shown. (B) Correlations among expression of each of the 24 V β structures among Ki-67⁺ and Ki-67⁻ cells were averaged for each patient and each control. Distributions of V β expression better correlated between Ki-67⁺ and Ki-67⁻ populations in the HIV-1⁺ ($n = 9$) subjects than among healthy controls ($n = 6$) by Spearman correlations. (C) Proportions of clones as identified by CDR3 sequencing among sorted noncycling (CD71⁻, x-axis) and cycling (CD71⁺, y-axis) memory CD8⁺ T cell populations in 3 healthy controls (top) and 3 HIV-1-infected patients (bottom). Each dot represents a unique clone identified by CDR3 segment sequencing. Red, blue, and green dots represent the clone frequencies in CD71⁺, CD71⁻/CD71⁺ (shared clones), and CD71⁻ cells, respectively. Analyses were performed using immunoSEQ analyzer software (Adaptive Biotechnologies). (D) Entropy (diversity) measurements in proliferating (CD71⁺) and nonproliferating (CD71⁻) memory CD8⁺ T cells in controls (CNT) and HIV-1-infected subjects (HIV-1).

T cells are granzyme B⁺ (Figure 4, A and B). As expected, in untreated HIV-1 infection the majority of HIV-1-reactive and CMV-reactive CD8⁺ T cells are granzyme B⁺, yet in untreated HIV-1-infected subjects, most influenza-reactive CD8⁺ T cells are also granzyme B⁺ (Figure 4, A and B). These data suggest that regardless of the state of the infection, persistent or remote, memory CD8⁺ T cells reactive to viral peptides frequently express granzyme B in people with untreated HIV-1 infection.

IL-15 drives memory CD8⁺ T cell cycling and granzyme B expression in vitro. To further investigate the hypothesis that memory CD8⁺ T cell activation, cycling, and expansion are largely driven by bystander mechanisms, we examined the effects of selected cytokines on memory CD8⁺ T cell cycling and phenotype. We examined the effects of 3 common γ chain receptor cytokines (IL-2, IL-7, and IL-15) known to drive T cell proliferation. We also examined the effects of 2 inflammatory cytokines (IL-1 β and IL-6) that are expressed at high levels in HIV-1 infection (19, 20) and that have been shown to induce variable degrees of T cell cycling and proliferation (20). Peripheral blood mononuclear cells (PBMCs) from healthy HLA-A*02:01 participants were incubated with concentrations of cytokines that we had previously demonstrated to be optimal for driving CD4⁺ T cell cycling and proliferation (20). We found that IL-15 and, to a lesser extent, IL-7 increased the proportion of CD8⁺ T cells expressing granzyme B (Figure 5, A and C), and this was particularly apparent among CD8⁺ T cells recognizing influenza or CMV peptides. Low-level CD8⁺ T cell cycling was induced in vitro by IL-7 exposure, while IL-15 induced substantial CD8⁺ T cell cycling (Figure 5, B and C), and, importantly, cycling induced by IL-15 was exaggerated among memory CD8⁺ T cells reactive with both CMV and influenza peptides. Thus, by exposing PBMCs to IL-15 in vitro, we were able to generate in vitro the cycling and potentially cytolytic phenotype of CD8⁺ T cells identified in HIV-1-infected patients.

IL-15 is highly expressed in the lymph nodes of untreated HIV-1-infected patients. Since IL-15 could induce in vitro a memory CD8⁺ T cell phenotype characteristic of untreated HIV-1 infection, we

examined IL-15 expression in the lymph nodes (LNs) of HIV-1-infected patients and HIV-1-uninfected controls. Patient characteristics are listed in Table 2. Shown in Figure 6A are representative IL-15 stains of LN sections from a healthy control, an HIV-1 viremic subject, and an HIV-1-infected patient with controlled viremia on ART. Summary data representing the proportional surface area of each node expressing IL-15 are shown in Figure 6B. Among 17 healthy controls, 22.5% \pm 3.1% (mean \pm SE) of the LN T cell zone area stained positively for IL-15 versus 40.3% \pm 4.9% in 13 viremic untreated patients ($P = 0.008$, Kruskal-Wallis test). Among the 12 ART-suppressed patients, 24.4% \pm 5.3% of the LN surface areas stained positively for IL-15, which was significantly lower than the staining seen in the nodes of viremic subjects ($P = 0.03$) but not different from the staining in healthy controls' LNs.

A potential role of IL-15 in CD8⁺ T cell expansion is suggested further by a significant positive correlation ($r = 0.582$, $P = 0.040$) between LN IL-15 levels and circulating CD8⁺ T cell numbers in the viremic patients (Figure 6C). We did not observe a correlation between plasma HIV-1 RNA levels and IL-15 expression in LNs of untreated patients (Supplemental Figure 2A), nor did we find a correlation between LN IL-15 levels and circulating CD8⁺ T cell numbers in healthy controls or ART-treated HIV-1 infection (Supplemental Figure 2, B and C, respectively).

Lastly, plasma levels of IL-15 did not correlate with peripheral CD8 T cell counts in the untreated cohort, the ART-treated patients, or the healthy controls (data not shown).

Discussion

Expansion of circulating CD8⁺ T cell numbers is characteristic in untreated HIV-1 infection; these numbers remain elevated even after years of suppressive ART, and in recent studies, persistent expansion of these cells has been linked to increased risk of morbidity and mortality (13, 21, 22). What then drives this expansion? Here we confirm profound increases in memory CD8⁺ T cell cycling in untreated HIV-1 infection (3, 13, 23–25) and show that CD8⁺ T cell cycling normalizes with suppression of HIV-1 replication. To identify the determinants of this increased cycling, we examined the diversity of the T cell repertoire in untreated infection and found that the V β distribution between cycling and noncycling memory CD8⁺ T cells was tightly correlated, and even better correlated in untreated HIV-1 infection than among healthy controls. More detailed characterization of T cell receptor diversity by deep sequencing of CDR3 regions confirmed that the cycling memory CD8 T cells in untreated HIV infection represented the diversity of the entire resting memory CD8 T cell repertoire. This suggests that although there may be greater and more sustained exposure to particular antigens that may skew the CD8⁺ T cell V β repertoire in acute HIV-1 infection (26, 27), most cycling in chronic HIV-1 infection is driven by bystander mechanisms and not by T cell receptor stimulation.

We then examined the cycling and granzyme B expression of memory CD8⁺ T cells reactive with peptides derived from both persistent (HIV-1 or CMV) and nonpersistent (influenza) pathogens. We found that in healthy controls, cycling of CMV- and influenza-reactive effector memory CD8⁺ T cells was comparable to or lower than the cycling frequency in the entire effector memory CD8⁺ T cell population, while in HIV-1 infection, there was enrichment

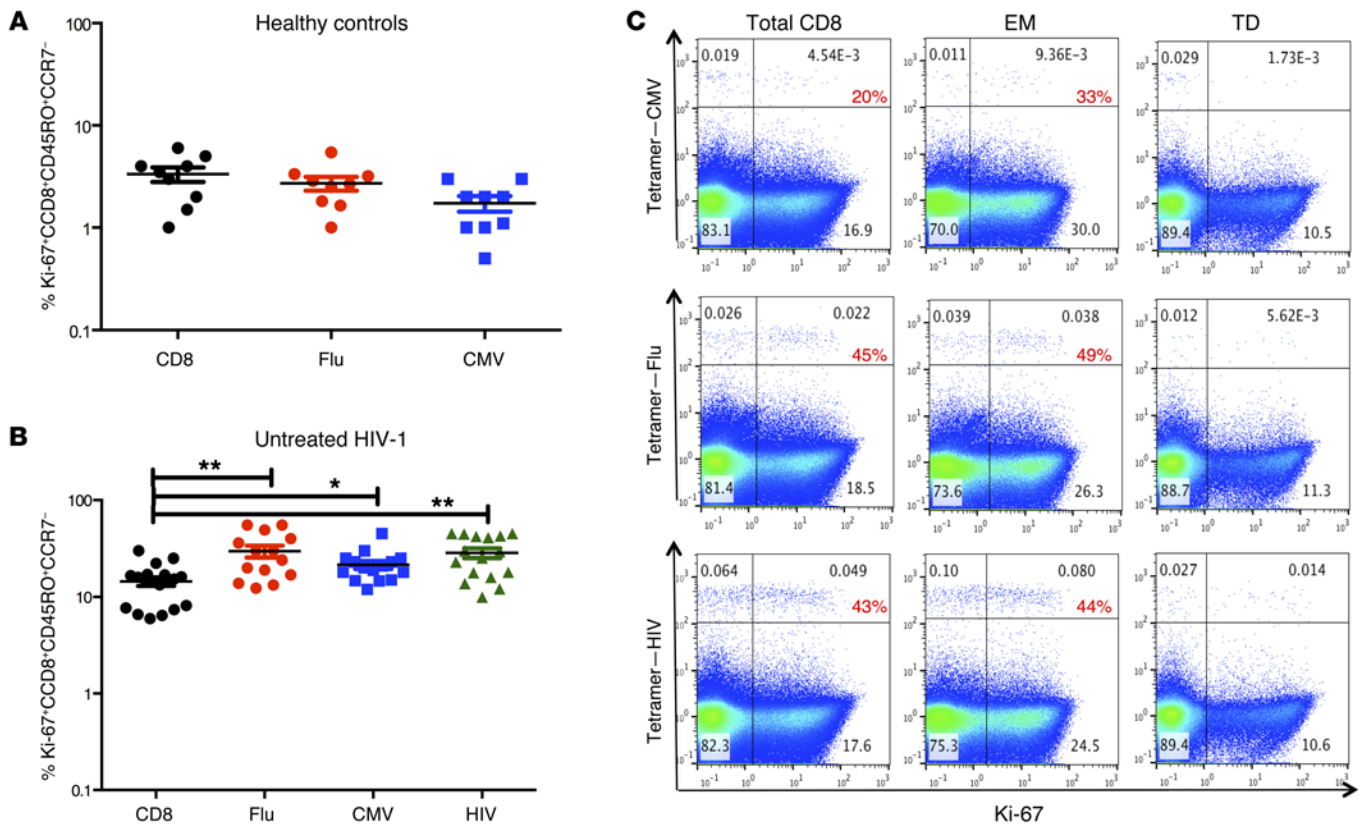


Figure 3. Increased cycling in CD8⁺ memory T cells that bind CMV, influenza, and HIV-1 peptide-tetramers in chronic untreated HIV-1 infection. (A and B) Percentages of Ki-67⁺ effector memory (EM) CD8⁺ T cells and EM CD8⁺ T cells binding influenza, CMV, and HIV-1 peptide-HLA-A*02:01 tetramer complexes in healthy controls (*n* = 9) (A) and HIV-1-infected patients (*n* = 20) (B). (C) Representative dot plots showing the frequencies of Ki-67 expression among CMV-, influenza-, and HIV-1-specific CD8 T cells as detected by peptide-tetramer complex binding among total CD8 T cells, among CCR7⁺CD45RO⁺ EM cells, and among terminally differentiated (TD) CCR7⁺CD45RO⁺ CD8 T cells in peripheral blood from an untreated patient. **P* < 0.05, ***P* < 0.01 by Kruskal-Wallis test. Percentages in red represent the frequency of Ki-67 expression among tetramer-peptide-binding cells.

of cycling among CD8⁺ T cells reactive with peptides derived from both persistent viruses (CMV and HIV-1), but there was also enrichment of cycling among memory CD8⁺ T cells reactive with peptides derived from influenza virus. This was not a consequence of recent exposure to influenza peptides, as within each group (patients and controls) the frequency of cycling among influenza-specific CD8 T cells was similar irrespective of timing of sample collection within or outside of the influenza season (data not shown). We found enrichment for granzyme B expression in CMV-reactive but not influenza-reactive memory CD8⁺ T cells of healthy controls, suggestive of ongoing exposure to CMV but not influenza in these subjects. In untreated HIV-1 infection, however, not only were CMV- and HIV-1-reactive memory CD8⁺ T cells enriched for granzyme B expression, but so also were influenza-reactive CD8⁺ T cells. These findings when taken together suggest that the increased cycling, CD8⁺ T cell expansion, and granzyme B expression in HIV-1 infection could be driven by bystander mechanisms. We show here that in vitro exposure to IL-15 induces both cycling and granzyme B expression in memory CD8⁺ T cells, and these effects were particularly enriched among cells with memory for these viral peptides.

Earlier studies in other settings have demonstrated an important role for IL-15 in the expansion of memory CD8⁺ T cells (28–30) and in the induction and maintenance of gran-

zyme B expression (31–33). We have previously reported a trend to increased production of supernatant IL-15 by LN histocultures of HIV-1-infected subjects (11). Increased *IL15* mRNA was found in alveolar macrophages (34, 35) and in blood myeloid dendritic cells of HIV-1-infected patients not receiving ART (35). Our study extends these earlier findings, placing them into context by providing strong evidence that IL-15 drives bystander memory CD8⁺ T cell expansion in HIV-1 infection, demonstrating high levels of IL-15 protein in LN sites of T cell maturation in untreated HIV-1-infected patients. This is important as post-transcriptional mechanisms are important regulators of IL-15 expression (36). We further demonstrate that LN IL-15 levels are correlated with in vivo circulating CD8⁺ T cell numbers and that ART normalizes both LN IL-15 levels and the frequency of CD8⁺ T cell cycling. T cell receptor repertoire analysis confirms the hypothesis that bystander mechanisms are major drivers of CD8⁺ T cell cycling during chronic HIV-1 infection. We were also able to recapitulate the high-level granzyme expression of memory CD8⁺ T cells seen in chronic HIV-1 infection by exposing PBMCs of healthy controls to IL-15 in vitro. We suspect that IL-7 is less important in this regard, as *IL7* RNA levels in these nodes were similar in all 3 subject groups (not shown), and T cell responsiveness to IL-7 is thought to be impaired in chronic

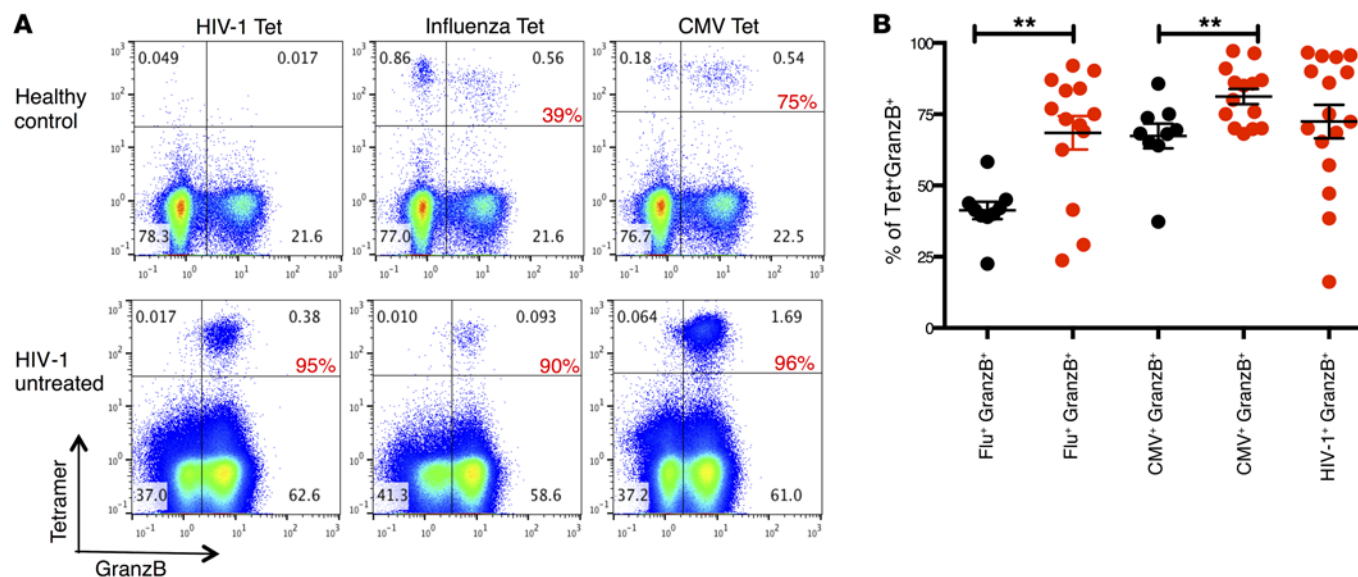


Figure 4. Increased granzyme B expression among peptide-tetramer-binding CD8⁺ T cells in chronic HIV-1 infection. CD8⁺ T cells from HLA-A*02:01⁺ patients and controls were examined for binding of HIV-1, influenza, and CMV peptide-tetramer complexes and for intracellular expression of granzyme B. **(A)** Representative data from a healthy control (upper panels) and a viremic HIV-1-infected (lower panels) patient. Percentages in red represent the frequency of tetramer-peptide-binding cells that are granzyme B⁺. **(B)** The proportions of granzyme B⁺ CD8 T cells in healthy controls (black circles, $n = 9$) and in the HIV-1-infected group (red circles) that bind peptide-tetramer complexes specific for influenza (Flu) ($n = 14$), CMV ($n = 14$), and HIV-1 ($n = 16$). ** $P < 0.01$ by Kruskal-Wallis test.

HIV infection as a result of LN fibrosis (37) and via inhibition of IL-7 signaling by inflammatory cytokines (20, 38, 39). Further studies are warranted to identify the cellular source of IL-15 that appears to drive memory CD8⁺ T cell activation and expansion in untreated HIV-1 infection. The diffuse IL-15 staining in our LN sections is consistent with a stromal cell source as suggested by murine studies (40), and the high levels of IL-15 expression in these tissues may help to drive tissue damage (41) and fibrosis (37, 42) that characterize chronic HIV-1 infection.

Not all memory CD8⁺ T cells are “authentic” memory cells derived from encounter with foreign antigen, as memory-phenotype cells can be generated after exposure of CD4⁺ (43, 44) and CD8⁺ T cells (45) to cytokines alone. We suspect that enrichment of viral peptide-reactive memory CD8⁺ T cells among cycling and granzyme B-expressing cells reflects the increased responsiveness of authentic memory CD8⁺ T cells (43) in response to IL-15 exposure in vivo as we have demonstrated in vitro. In this regard, we and others have recently shown that HIV-1-infected people who are also CMV-coinfected have higher circulating CD8 T cell numbers than do CMV-seronegative patients (46, 47). In light of our demonstration that effector memory cells with memory for viral peptides demonstrate a heightened cycling response to IL-15, it may not be surprising that chronic infection with CMV that typically commands a substantial proportion of the T cell repertoire (8, 48) is associated with profound CD8⁺ T cell expansion in chronic HIV-1 infection. A proposed model of CD8 T cell expansion in chronic HIV-1 infection is shown in Figure 7. Upon HIV-1 infection an IL-15 “danger signal” (41) is induced in the LNs, increasing the cytolytic potential and numbers of CD8⁺ T cells, especially CMV-specific effector memory CD8 T cells that persist even after HIV-1 replication is controlled by ART.

What drives increased LN IL-15 expression in chronic HIV-1 infection? Although we could not find a correlation between IL-15 expression and plasma HIV-1 RNA levels, HIV-1 can induce IL-15 expression via TLR 7/8 ligation (49), and in chronic HIV-1 infection, increased gut mucosal barrier permeability permits systemic translocation of microbial products (50, 51) and their localization in lymphoid tissues (52) that also can induce expression of IL-15 (35). Further research is needed to understand better how CD8⁺ T numbers are maintained at high levels even after years of therapy as well as how persistent CD8⁺ T cell expansion during chronic HIV-1 infection is associated with increased morbidity and mortality (13, 21, 22).

Methods

Study subjects. Two separate cohorts were studied. The first, in which we analyzed CD8 T cell responses, is described in Table 1. A second cohort, in which LN IL-15 was examined, is described in Table 2.

The HLA-A*02:01 HIV-1-infected therapy-naive patients ($n = 20$) had a median plasma HIV-1 RNA level of 210,000 (range 50,000–420,000) copies/ml and median CD4⁺ T cell counts of 414 cells/μl. Elderly healthy control patients were all more than 70 years old. HIV-1-infected immune success (IS) ($n = 12$) and immune failure (IF) patients had median CD4 T cell counts of 610 cells/μl (range 449–830) and 249 cells/μl (range 180–308), respectively. IS and IF patients were all receiving combination ART with plasma levels of HIV-1 RNA less than 50 copies/ml.

LNs were obtained from 17 control donors (median age 50, 9 male, 8 female). Inguinal LNs were obtained from 16 donors by inguinal resection under local anesthesia. One control pelvic node was obtained during clinically indicated pelvic surgery. Inguinal nodes were obtained from 13 HIV-1⁺ infected untreated patients

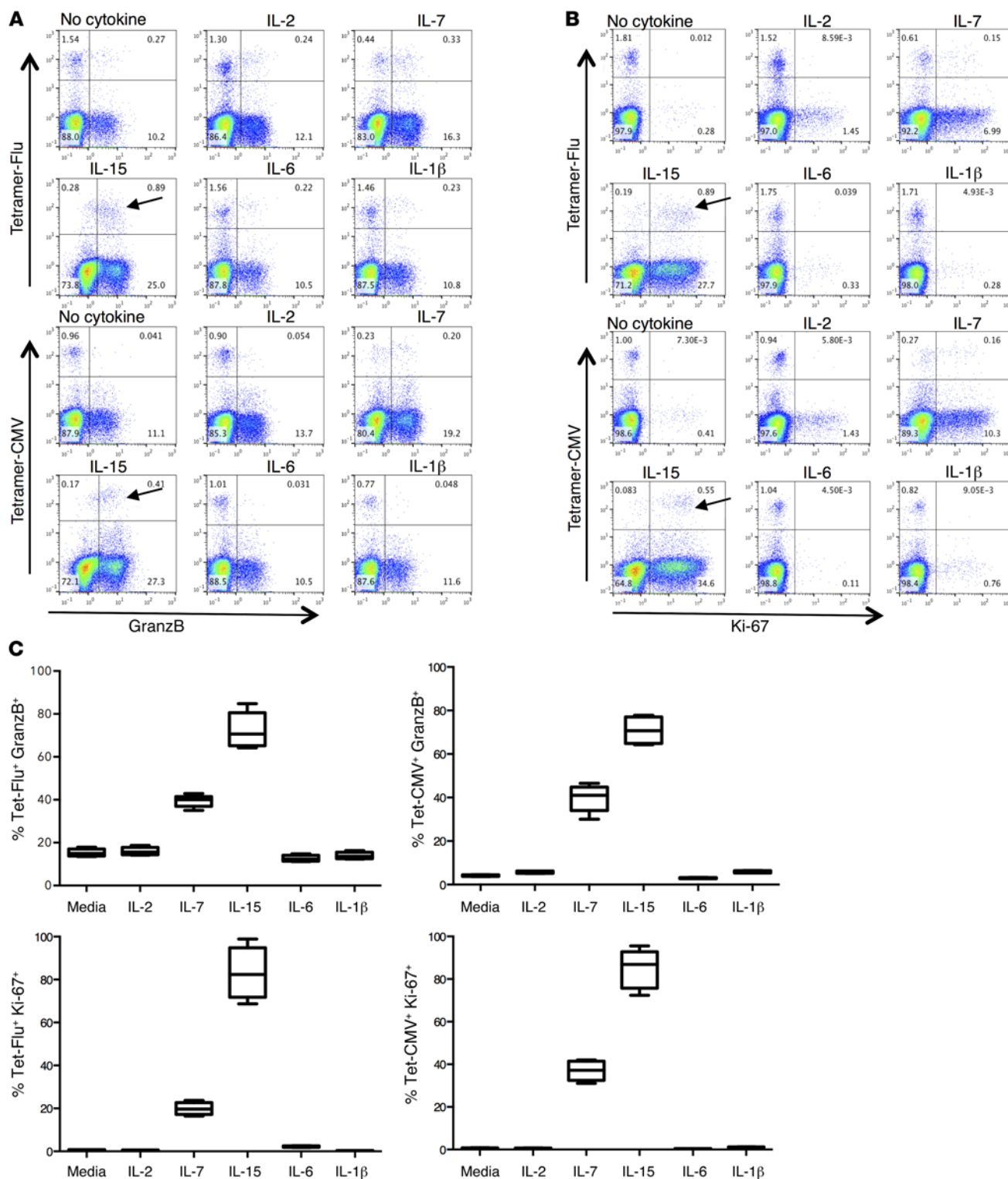


Figure 5. IL-15 induces cell cycling and granzyme B expression in CD8⁺ T cells. (A and B) PBMCs from HLA-A*02:01 healthy subjects were incubated for 48 hours with IL-2 (50 ng/ml), IL-7 (10 ng/ml), IL-15 (20 ng/ml), IL-6 (10 ng/ml), or IL-1β (10 ng/ml), then stained for expression of CD3, CD8, binding of CMV or influenza peptide-tetramer complexes, and either granzyme B (A) or Ki-67 (B). (C) Box plot summary data showing the medians, interquartile ranges, and minimum/maximum proportions of tetramer-peptide-binding CD8⁺ T cells that are granzyme B⁺ or Ki-67⁺ among 5 HLA-A*02:01 healthy control donors after 48 hours of incubation with the indicated cytokines.

Table 2. Patients in whom lymph node biopsies were obtained

	<i>n</i>	Age ^A	Gender	ART	Plasma HIV-1 RNA ^B	CD4 ^C	CD8 ^D	Class I haplotype
Healthy controls	17	50 (28–74)	9 male, 8 female	Negative	NA	789 (675–1,124)	305 (160–635)	ND
HIV-1 ⁺ untreated	13	34 (24–51)	10 male, 3 female	Negative	20,499 (167–120,469)	602 (207–1,185)	686 (345–120)	ND
HIV-1 ⁺ on ART	12	47 (27–59)	11 male, 1 female	Positive	46 (20–149)	539 (132–980)	946 (500–1,659)	ND

^AMedian age (min.–max.); ^Bmedian plasma HIV-1 RNA (min.–max.); ^Cmedian peripheral CD4 T cell count (min.–max.); ^Dmedian peripheral CD8 T cell count (min.–max.). NA, not applicable; ND, not determined.

(median age 34, 10 male, 3 female) and 12 HIV-1-infected patients on ART (median age 47, 11 male, 1 female). Patient characteristics are detailed in Table 2.

MHC class I tetramers. BV421-labeled MHC class I HLA-A*02:01 tetramers were obtained from the NIH Tetramer Facility (Atlanta, GA). Tetramers were loaded with the pp65 CMV peptide NLVPM-VATV, the influenza matrix peptide GILGFVFTL, and the HIV-1 pol peptide ILKEPVHGV.

MHC class I haplotyping. HLA typing was performed using single specific primer-polymerase chain reaction (SSP-PCR) low/high-resolution conventional genotyping kits (QIAamp Kit; QIAGEN). In brief, DNA was extracted from blood using the QIAamp 96 blood kit followed by an intermediate-resolution sequence-specific oligonucleotide probe PCR (SSOP-PCR) typing and high-resolution SSP-PCR subtyping (53).

Flow cytometry. Cells were stained with fluorochrome-labeled monoclonal antibodies at 4°C for 30 minutes or with peptide-tetramer complexes for 1 hour at 37°C. After surface staining, cells were washed,

fixed, and permeabilized using Cytotfix/Cytoperm (catalog 554714; BD) following the manufacturer’s protocol. The following antibody conjugates were used: anti-CD3-Percp (clone SK7, catalog 347344; BD), anti-CD8-APCcy7 (clone SK1, catalog 557834; BD), anti-CD45RO-FITC (clone UCHL1, catalog 555492; BD), Ki-67-PE (clone B56, catalog 561283; BD), anti-CCR7-PE-cy7 (clone 3D12, catalog 557648; BD), and anti-granzyme B-Alexa 647 (clone GB11, catalog 560212; BD). After staining, samples were examined by flow cytometry (Quant; Miltenyi Biotec) and analyzed using FlowJo software (Tree Star). Anti-CD71-PE antibody (clone M-A712, catalog 555537; BD) was used for cell sorting.

Cell culture. All PMBCs were derived from peripheral blood sampling. PMBCs were isolated from peripheral blood or apheresis donor packs by sodium diatrizoate density centrifugation (Amersham Biosciences). Samples were cryopreserved using FBS (Gemini Bioproducts) supplemented with 10% DMSO. Cryopreserved samples were maintained in liquid nitrogen (gas phase) and thawed for subsequent usage. Recombinant human cytokines—IL-2 catalog AFL202, IL-7 cat-

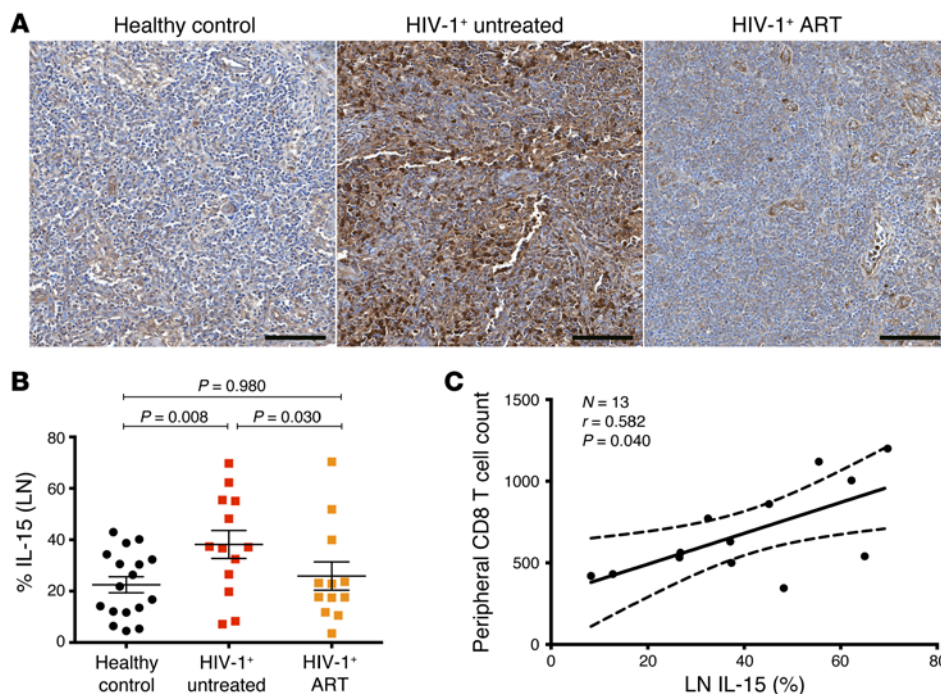


Figure 6. Increased IL-15 expression in LNs of untreated HIV-1-infected patients. (A) Representative IHC images of LN sections obtained from an HIV-1 control subject (left), an HIV-1-infected viremic patient (middle), and an HIV-1-infected ART-suppressed patient (right). IL-15 staining (brown), hematoxylin nuclear counterstain (blue). Scale bar: 100 μM. (B) Summary data (means and SEM) representing percentage surface area of the T cell zone that stained for IL-15 protein in 17 healthy controls, 13 HIV-1 untreated, and 12 HIV-1 ART-treated patients. *P* values were determined by Kruskal-Wallis test. (C) Spearman correlations between the LN levels of IL-15 and peripheral CD8⁺ T cell counts in untreated HIV-1-infected patients.

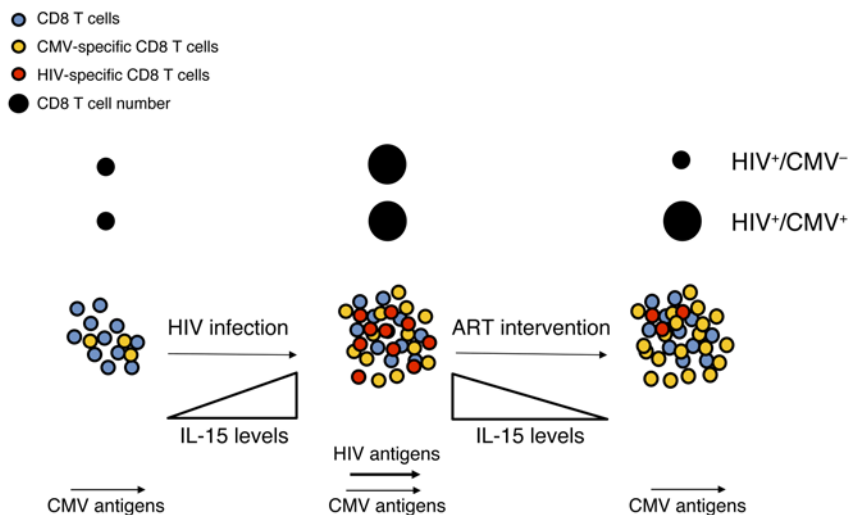


Figure 7. Model for CD8 T cell expansion in chronic HIV-1 infection. During untreated HIV-1 infection, levels of IL-15 increase in the LNs, inducing bystander activation of CD8 T cells and expanding HIV-1-reactive and other memory CD8 T cells (e.g., CMV specific). Following ART intervention, levels of HIV-1 fall, as do levels of IL-15, but CMV antigens persist, allowing the maintenance of CMV-specific CD8 T cells previously expanded by IL-15 exposure before ART. The size of the CD8 T cell pool remains elevated even on ART as illustrated by the black circles in HIV⁺/CMV⁻ coinfecting but not in HIV⁺/CMV⁻ or HIV⁻/CMV⁺ patients (41).

along AFL207, IL-15 catalog 247-ILB, IL-1 β catalog AFL201, and IL-6 AFL206—were all obtained from R&D Systems.

V β distribution analysis. Identification of T cells expressing different V β T cell receptor chains was performed using the IOTest Beta Mark TCR V β Kit (catalog IM3497; Coulter). Frozen PBMCs were thawed in RPMI supplemented with 10% human serum, rested for 1 hour at 37°C, and stained with anti-CD8-APCcy7 (BD), anti-CD3-Per-cp (BD), BV421 anti-CD45RO (clone UCHL1, catalog 562641; BD), rat anti-human CCR7-PEcy7 (BD), and the commercial panel of 24 anti-V β antibodies recognizing V β 1, V β 2, V β 3, V β 4, V β 5.1, V β 5.2, V β 5.3, V β 7.1, V β 7.2, V β 8, V β 9, V β 11, V β 12, V β 13.1, V β 13.2, V β 13.6, V β 14, V β 16, V β 17, V β 18, V β 20, V β 21.3, V β 22, and V β 23, each linked to FITC, PE, or both. Cells were then fixed and permeabilized (BD) and stained with anti-Ki-67-Alexa 647 (clone B56, catalog 558615; BD).

CDR3 sequencing. We have established that the cell surface transferrin receptor CD71 is a near-perfect surrogate for Ki-67 (Supplemental Figure 1), making it possible to sort live, unfixed, proliferating CD8 T cells. Thus, 60,000 CD71-CD45RO⁺CCR7⁻ and CD71⁺CD45RO⁺CCR7⁻ CD8⁺ T cells from 3 HIV-1-infected viremic patients and 3 healthy donors were FACS-sorted (BD FACSAria). Purity was greater than 90%. CDR3 regions of the V β segments were deep-sequenced and analyzed using immunoseq analyzer software (Adaptive Biotechnologies). See *Statistics* below for calculation of entropy.

IHC staining for IL-15. Inguinal LNs were obtained by surgical resection and fixed in paraformaldehyde (4%), followed by embedding in paraffin blocks. IHC staining using mouse anti-human IL-15 (clone BDI150, catalog ABIN235712; Antibodies-Online) was performed using a biotin-free polymer approach (mouse Polink-2; Golden Bridge International) on 5- μ m tissue sections mounted on glass slides, dewaxed, and rehydrated with double-distilled water. Antigen retrieval was performed by heating of sections in 10 mM citrate buffer, pH 4.0 (Golden Bridge International), in a pressure cooker (Decloaking Chamber model DC2002; Biocare Medical) at 122°C for 30 seconds. After cooling of slides and washing in double-distilled H₂O, slides were incubated with proteinase K (2.0 μ g/ml in 20 mM Tris-HCl containing 2 mM CaCl₂; Fisher Scientific) for 15 minutes at room temperature. Tissue sections were incubated with 1.5% (vol/vol) H₂O₂ in Tris-buffered saline (TBS) (pH 7.4) for 10 minutes to block endogenous peroxidases and then incubated in blocking buffer (TBS with 0.05% Tween-20 and 0.5%

casein) for 10 minutes. Tissue sections were incubated with mouse anti-human mature IL-15 (clone BDI150; Antibodies-Online) diluted in blocking buffer overnight at 4°C. Tissue sections were washed, and the mouse Polink-2 staining system (Golden Bridge International) was used according to the manufacturer's recommendations. Sections were developed with Impact 3,3-diaminobenzidine (Vector Laboratories), counterstained with hematoxylin, and mounted in Permount (Fisher Scientific). Stained slides were scanned at high magnification (\times 200) with ScanScope AT2 System (Aperio Technologies), yielding high-resolution data for the entire tissue section. Representative regions of interest (500 μ m²) were identified and high-resolution images extracted from whole-tissue scans. The percentage of the LN area that stained for IL-15 was quantified using Photoshop CS5 (Adobe) and Fovea tools.

Statistics. Group variables were compared with the Kruskal-Wallis test with post-hoc Dunn-Bonferroni pairwise comparisons, adjusted to a family-wise alpha error of 0.05; or Mann-Whitney *U* tests using GraphPad Prism software. *P* values \leq 0.05 were considered statistically significant. The comparison of V β distributions between Ki-67⁺ and Ki-67⁻ cells was performed as follows: for each subject we performed a Spearman correlation between the frequencies of each V β family in the cycling (Ki-67⁺) and noncycling (Ki-67⁻) cells.

Entropy $H(X)$ was calculated by a Shannon entropy calculation where $H(X) = -1 \cdot \sum P(x) \log_2 [P(x)]$. For a productive in-frame sequence x , $P(x)$ = sequence count/total productive count. Greater entropy values reflect greater diversity.

Study approval. This study was approved by the IRB at University Hospitals/Case Medical Center, and written informed consent was obtained from all patients.

Author contributions

S-AY designed, performed, and analyzed experiments and, together with SFS and MML, wrote the manuscript. CLS, MLF, and SP performed and analyzed experiments and helped to write the manuscript. JDE and JA generated the LN data. RLD and JMJ provided LN tissues. AR and MPD performed statistical analysis. JMM, PWH, SAL, and SSV contributed to writing the manuscript. DHC and BR provided patient PBMCs. All authors contributed to general design and discussion of the project and reviewed and approved the manuscript.

Acknowledgments

We acknowledge the NIH Tetramer Core Facility (contract HHSN272201300006C) for provision of the tetramers. This work was supported by grant awards AI105937 and AI68636 from the NIAID; the Fasenmyer Foundation; NIAID grant award AI36219; and the Case Western Reserve University Center for AIDS Research. This project has been funded in part with federal funds from the National Cancer Institute, NIH, under contract no. HHSN261200800001E. The content of this publication does

not necessarily reflect the views or policies of the Department of Health and Human Services, nor does mention of trade names, commercial products, or organizations imply endorsement by the US government.

Address correspondence to: Michael M. Lederman, Case Western Reserve University School of Medicine, 2061 Cornell Road, Cleveland, Ohio 44106, USA. Phone: 216.844.8786; E-mail: lederman.michael@clevelandactu.org.

- Hellerstein MK, McCune JM. T cell turnover in HIV-1 disease. *Immunity*. 1997;7(5):583-589.
- Kovacs JA, et al. Identification of dynamically distinct subpopulations of T lymphocytes that are differentially affected by HIV. *J Exp Med*. 2001;194(12):1731-1741.
- Hazenber MD, et al. T-cell division in human immunodeficiency virus (HIV)-1 infection is mainly due to immune activation: a longitudinal analysis in patients before and during highly active antiretroviral therapy (HAART). *Blood*. 2000;95(1):249-255.
- Boffill M, et al. Increased numbers of primed activated CD8⁺CD38⁺CD45RO⁺ T cells predict the decline of CD4⁺ T cells in HIV-1-infected patients. *AIDS*. 1996;10(8):827-834.
- Deeks SG, et al. Immune activation set point during early HIV infection predicts subsequent CD4⁺ T-cell changes independent of viral load. *Blood*. 2004;104(4):942-947.
- Hazenber MD, et al. Persistent immune activation in HIV-1 infection is associated with progression to AIDS. *AIDS*. 2003;17(13):1881-1888.
- Wilson CM, Ellenberg JH, Douglas SD, Moscicki AB, Holland CA, Reach Project Of The Adolescent Medicine HIV/AIDS Research Network. CD8⁺CD38⁺ T cells but not HIV type 1 RNA viral load predict CD4⁺ T cell loss in a predominantly minority female HIV⁺ adolescent population. *AIDS Res Hum Retroviruses*. 2004;20(3):263-269.
- Betts MR, et al. Analysis of total human immunodeficiency virus (HIV)-specific CD4(+) and CD8(+) T-cell responses: relationship to viral load in untreated HIV infection. *J Virol*. 2001;75(24):11983-11991.
- Migueles SA, et al. HIV-specific CD8⁺ T cell proliferation is coupled to perforin expression and is maintained in nonprogressors. *Nat Immunol*. 2002;3(11):1061-1068.
- Gea-Banacloche JC, et al. Maintenance of large numbers of virus-specific CD8⁺ T cells in HIV-infected progressors and long-term nonprogressors. *J Immunol*. 2000;165(2):1082-1092.
- Biancotto A, et al. Abnormal activation and cytokine spectra in lymph nodes of people chronically infected with HIV-1. *Blood*. 2007;109(10):4272-4279.
- Chen G, et al. CD8 T cells specific for human immunodeficiency virus, Epstein-Barr virus, and cytomegalovirus lack molecules for homing to lymphoid sites of infection. *Blood*. 2001;98(1):156-164.
- Serrano-Villar S, et al. HIV-infected individuals with low CD4/CD8 ratio despite effective antiretroviral therapy exhibit altered T cell subsets, heightened CD8⁺ T cell activation, and increased risk of non-AIDS morbidity and mortality. *PLoS Pathog*. 2014;10(5):e1004078.
- Migueles SA, et al. Lytic granule loading of CD8⁺ T cells is required for HIV-infected cell elimination associated with immune control. *Immunity*. 2008;29(6):1009-1021.
- Jiang W, et al. Cycling memory CD4⁺ T cells in HIV disease have a diverse TCR repertoire a phenotype consistent with bystander activation. *J Virol*. 2014;88(10):5369-5380.
- Carbonari M, et al. Comparison of the Vbeta repertoire in peripheral blood and in lymph nodes of HIV-infected subjects reveals skewed usage predominantly in CD8⁺ T cells. *Clin Immunol Immunopathol*. 1996;81(2):200-209.
- Giacoa-Gripp CB, Neves I Jr, Galhardo MC, Morgado MG. Flow cytometry evaluation of the T-cell receptor Vbeta repertoire among HIV-1 infected individuals before and after antiretroviral therapy. *J Clin Immunol*. 2005;25(2):116-126.
- Grant M, Pardoe I, Whaley M, Montaner JS, Hargigan PR. The T cell receptor Vβ repertoire shows little change during treatment interruption-related viral rebound in chronic HIV infection. *AIDS*. 2002;16(2):287-290.
- Tenorio AR, et al. Soluble markers of inflammation and coagulation but not T-cell activation predict non-AIDS-defining morbid events during suppressive antiretroviral treatment. *J Infect Dis*. 2014;210(8):1248-1259.
- Shive CL, et al. Inflammatory cytokines drive CD4⁺ T-cell cycling and impaired responsiveness to interleukin 7: implications for immune failure in HIV disease. *J Infect Dis*. 2014;210(4):619-629.
- Lee SA, et al. Impact of HIV on CD8⁺ T cell CD57 expression is distinct from that of CMV and aging. *PLoS One*. 2014;9(2):e89444.
- Lee SA, et al. Low proportions of CD28⁺ CD8⁺ T cells expressing CD57 can be reversed by early ART initiation and predict mortality in treated HIV infection. *J Infect Dis*. 2014;210(3):374-382.
- Giorgi JV, et al. Shorter survival in advanced human immunodeficiency virus type 1 infection is more closely associated with T lymphocyte activation than with plasma virus burden or virus chemokine coreceptor usage. *J Infect Dis*. 1999;179(4):859-870.
- Sousa AE, Carneiro J, Meier-Schellersheim M, Grossman Z, Victorino RM. CD4 T cell depletion is linked directly to immune activation in the pathogenesis of HIV-1 and HIV-2 but only indirectly to the viral load. *J Immunol*. 2002;169(6):3400-3406.
- Doisne JM, et al. CD8⁺ T cells specific for EBV, cytomegalovirus, and influenza virus are activated during primary HIV infection. *J Immunol*. 2004;173(4):2410-2418.
- Pantaleo G, et al. Major expansion of CD8⁺ T cells with a predominant Vβ usage during the primary immune response to HIV. *Nature*. 1994;370(6489):463-467.
- Pantaleo G, et al. Evidence for rapid disappearance of initially expanded HIV-specific CD8⁺ T cell clones during primary HIV infection. *Proc Natl Acad Sci U S A*. 1997;94(18):9848-9853.
- Alves NL, Hooibrink B, Arosa FA, van Lier RA. IL-15 induces antigen-independent expansion and differentiation of human naive CD8⁺ T cells in vitro. *Blood*. 2003;102(7):2541-2546.
- Liu K, Catalfamo M, Li Y, Henkart PA, Weng NP. IL-15 mimics T cell receptor crosslinking in the induction of cellular proliferation, gene expression, and cytotoxicity in CD8⁺ memory T cells. *Proc Natl Acad Sci U S A*. 2002;99(9):6192-6197.
- Weng NP, Liu K, Catalfamo M, Li Y, Henkart PA. IL-15 is a growth factor and an activator of CD8 memory T cells. *Ann N Y Acad Sci*. 2002;975:46-56.
- Tamang DL, Redelman D, Alves BN, Vollger L, Bethley C, Hudig D. Induction of granzyme B and T cell cytotoxic capacity by IL-2 or IL-15 without antigens: multiclonal responses that are extremely lytic if triggered and short-lived after cytokine withdrawal. *Cytokine*. 2006;36(3-4):148-159.
- Correia MP, Costa AV, Uhrberg M, Cardoso EM, Arosa FA. IL-15 induces CD8⁺ T cells to acquire functional NK receptors capable of modulating cytotoxicity and cytokine secretion. *Immunobiology*. 2011;216(5):604-612.
- Sandau MM, Kohlmeier JE, Woodland DL, Jameson SC. IL-15 regulates both quantitative and qualitative features of the memory CD8 T cell pool. *J Immunol*. 2010;184(1):35-44.
- Agostini C, et al. Interleukin-15 triggers activation and growth of the CD8 T-cell pool in extravascular tissues of patients with acquired immunodeficiency syndrome. *Blood*. 1997;90(3):1115-1123.
- Bastidas S, Graw F, Smith MZ, Kuster H, Günthard HF, Oxenius A. CD8⁺ T cells are activated in an antigen-independent manner in HIV-infected individuals. *J Immunol*. 2014;192(4):1732-1744.
- Waldmann TA, Tagaya Y. The multifaceted regulation of interleukin-15 expression and the role of this cytokine in NK cell differentiation and host response to intracellular pathogens. *Annu Rev Immunol*. 1999;17:19-49.
- Zeng M, et al. Cumulative mechanisms of lymphoid tissue fibrosis and T cell depletion in HIV-1 and SIV infections. *J Clin Invest*. 2011;121(3):998-1008.

38. Shive CL, et al. Inflammation perturbs the IL-7 axis, promoting senescence and exhaustion that broadly characterize immune failure in treated HIV infection. *J Acquir Immune Defic Syndr*. 2016;71(5):483–492.
39. Nguyen TP, et al. Interferon- α inhibits CD4 T cell responses to interleukin-7 and interleukin-2 and selectively interferes with Akt signaling. *J Leukoc Biol*. 2015;97(6):1139–1146.
40. Cui G, et al. Characterization of the IL-15 niche in primary and secondary lymphoid organs in vivo. *Proc Natl Acad Sci U S A*. 2014;111(5):1915–1920.
41. Jabri B, Abadie V. IL-15 functions as a danger signal to regulate tissue-resident T cells and tissue destruction. *Nat Rev Immunol*. 2015;15(12):771–783.
42. Estes JD, Haase AT, Schacker TW. The role of collagen deposition in depleting CD4⁺ T cells and limiting reconstitution in HIV-1 and SIV infections through damage to the secondary lymphoid organ niche. *Semin Immunol*. 2008;20(3):181–186.
43. Sprent J, Surh CD. Normal T cell homeostasis: the conversion of naive cells into memory-phenotype cells. *Nat Immunol*. 2011;12(6):478–484.
44. Younes SA, Punkosdy G, Caucheteux S, Chen T, Grossman Z, Paul WE. Memory phenotype CD4 T cells undergoing rapid, nonburst-like, cytokine-driven proliferation can be distinguished from antigen-experienced memory cells. *PLoS Biol*. 2011;9(10):e1001171.
45. Sosinowski T, et al. CD8 α^+ dendritic cell trans presentation of IL-15 to naive CD8⁺ T cells produces antigen-inexperienced T cells in the periphery with memory phenotype and function. *J Immunol*. 2013;190(5):1936–1947.
46. Freeman ML, et al. CD8 T cell expansion inflammation linked to CMV co-infection in ART-treated HIV infection. *Clin Infect Dis*. 2015;62(3):392–396.
47. Barrett L, Stapleton SN, Fudge NJ, Grant MD. Immune resilience in HIV-infected individuals seronegative for cytomegalovirus. *AIDS*. 2014;28(14):2045–2049.
48. Naeger DM, et al. Cytomegalovirus-specific T cells persist at very high levels during long-term antiretroviral treatment of HIV disease. *PLoS One*. 2010;5(1):e8886.
49. Dominguez-Villar M, Gautron AS, de Marcken M, Keller MJ, Hafler DA. TLR7 induces anergy in human CD4(+) T cells. *Nat Immunol*. 2015;16(1):118–128.
50. Brenchley JM, et al. Microbial translocation is a cause of systemic immune activation in chronic HIV infection. *Nat Med*. 2006;12(12):1365–1371.
51. Jiang W, et al. Plasma levels of bacterial DNA correlate with immune activation and the magnitude of immune restoration in persons with antiretroviral-treated HIV infection. *J Infect Dis*. 2009;199(8):1177–1185.
52. Estes JD, et al. Damaged intestinal epithelial integrity linked to microbial translocation in pathogenic simian immunodeficiency virus infections. *PLoS Pathog*. 2010;6(8):e1001052.
53. Younes SA, et al. HIV-1 viremia prevents the establishment of interleukin 2-producing HIV-specific memory CD4⁺ T cells endowed with proliferative capacity. *J Exp Med*. 2003;198(12):1909–1922.